International Journal of Nanomedicine

Dovepress
Taylor & Francis Group

Open Access Full Text Article

ORIGINAL RESEARCH

Daidzein-Decorated Gold Nanoparticles as a Novel Antimicrobial Strategy Against Carbapenem-Resistant Enterobacteriaceae

Juan Pan[1], Jia Zhang[2], Panjie Hu[1], Zhuocheng Yao[1], Xiaotuan Zhang[1,3], Tieli Zhou[1], Mo Shen[1]

[1]Department of Clinical Laboratory, The First Affiliated Hospital of Wenzhou Medical University Key Laboratory of Clinical Laboratory Diagnosis and Translational Research of Zhejiang Province, Wenzhou, Zhejiang, 325000, People's Republic of China; [2]School of Laboratory Medicine and Life Science, Wenzhou Medical University, Wenzhou, People's Republic of China; [3]Department of Clinical Laboratory, The Second Affiliated Hospital, Hengyang Medical School, University of South China, Hengyang, People's Republic of China

Correspondence: Mo Shen; Tieli Zhou, Department of Clinical Laboratory, The First Affiliated Hospital of Wenzhou Medical University, Key Laboratory of Clinical Laboratory Diagnosis and Translational Research of Zhejiang Province, Wenzhou, Zhejiang, 325000, People's Republic of China, Email shenmo601@163.com; wyztli@163.com

Introduction: Bacterial resistance to carbapenems is on the rise, and the failure of common antimicrobials poses a serious challenge in treating infections caused by drug-resistant strains. In this scenario, nanomaterials have received widespread attention in medicine.

Methods: In this study, the activity of daidzein-decorated gold nanoparticles (Daidzein_Au NPs) against carbapenem-resistant Enterobacteriaceae (CRE) strains was validated via in vivo and in vitro experiments, such as the microdilution broth method, growth curves, time-killing assays, and an abdominal infection model in mice. The potential mechanisms involved were examined using fluorescence quantification of N-phenyl-1-naphthylamine, propidium iodide, and reactive oxygen species (ROS) levels and transcriptomic analysis.

Results: Face-centered cubic Daidzein_Au NPs with an average size of 25.78 nm and a negative surface charge were successfully synthesized. The minimum inhibitory concentration (MIC) of Daidzein_Au NPs against the tested CRE strains was 8–16 μg/mL, and they exerted a good antimicrobial effect during the dynamic killing process. In vivo experiments showed that Daidzein_Au NPs can significantly enhance the survival rate (100%) and reduce the colony load of ascites in mice ($P < 0.05$). Furthermore, Daidzein_Au NPs destroyed the permeability of bacterial cell membranes, increased the production of ROS ($P < 0.05$), and affected the metabolism of CRE strains to play a role in killing.

Conclusion: Daidzein_Au NPs exhibit excellent antibacterial activity and are expected to become a promising solution to the threats posed by CRE strains.

Keywords: Daidzein, gold nanoparticles, carbapenem-resistant Enterobacteriaceae, antibacterial mechanism

Introduction

The abuse of antimicrobial agents has promoted the evolution of bacterial resistance, which has become a significant global public health threat.[1] In recent decades, the emergence and spread of multidrug-resistant (MDR) and extensively drug-resistant (XDR) Enterobacteriaceae have endangered public health.[2] Carbapenems, which are *β*-lactams with broad-spectrum antimicrobial effects, are one of the drugs of choice for treating MDR bacterial infections.[3] Carbapenems have been proven to be valuable in treating severe Gram-negative bacterial and polymicrobial mixed infections.[4] However, in 2017, the World Health Organization listed carbapenem-resistant Enterobacteriaceae (CRE) as one of the top three drug-resistant bacteria globally.[5] Carbapenem resistance can exert devastating effects as these agents are often the last line of defense against drug-resistant bacteria.

The resistance mechanism of CRE is predominantly attributed to the production of carbapenemases, with *Klebsiella pneumoniae* carbapenemase (KPC) and New Delhi metallo-*β*-lactamase (NDM) being the most common ones.[6,7] The genes encoding these enzymes often coexist with multiple antimicrobial resistance genes, resulting in the MDR phenotype of these

Received: 5 February 2025
Accepted: 9 June 2025
Published: 19 June 2025

Graphical Abstract

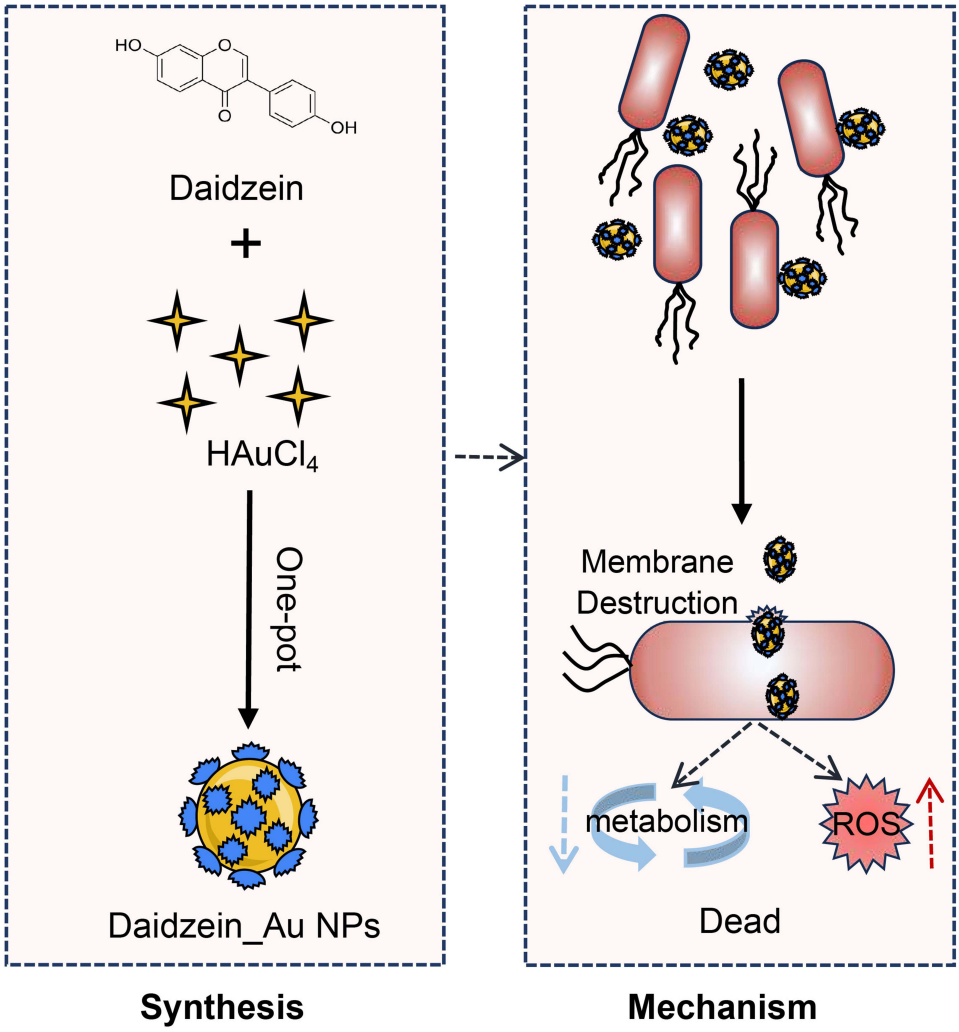

bacteria, which limits the selection of effective antimicrobial agents. In addition, such resistance-encoding genes are often transferred horizontally between clinical strains, leading to the spread of drug-resistant bacteria and causing a global health crisis.[8] Moreover, CRE has a propensity for MDR and is associated with a high mortality rate in bloodstream infections. Hence, CRE is classified as the highest threat level.[3,9] In recent years, the prevalence of CRE in China has increased. According to China's national bacterial surveillance data, the resistance rate of Enterobacteriaceae to imipenem (IMP) and meropenem (MEM) has risen markedly since 2016. MEM-resistant *K. pneumoniae* has reached 24.2%, with the 2020 resistance rate increasing by >60% compared with that of 2015.[10] The resistance rate to carbapenems is rising; therefore, identifying new therapeutic options is crucial.

Nanotechnology offers a cutting-edge solution to today's pressing challenges,[11] and nanoparticles, typically ranging in size from 0.2 to 100 nm, can be an effective novel antimicrobial strategy. Of the various nanoparticles, gold nanoparticles (Au NPs) are the most effective and biocompatible.[12] Traditionally, chemical and physical methods have been used to synthesize Au NPs, but their use is associated with the disadvantages of relying on highly toxic reagents, polluting the environment, and requiring expensive equipment.[13,14] Thus, there is a growing interest in "green" synthesis, where biological extracts (bacteria, fungi, plants, etc) are added drop by drop to $HAuCl_4$ salt solution and mixed thoroughly to initiate Au NPs synthesis,[15] with plant-based metal nanoparticle synthesis being the most popular. Plant-

based Au NPs exhibit unique application advantages across multiple fields owing to their small and uniform particle size. In addition, their high surface-area-to-volume ratio substantially enhances drug loading efficiency and enables precise targeted delivery.[16] These nanoparticles can effectively conjugate with biomolecules such as proteins and nucleic acids, making them appropriate agents for gene therapy and in vitro diagnostics.[17] Metal nanoparticles, especially Au NPs, exhibit diversified catalytic activities, such as catalyzing the decomposition of hydrogen peroxide and producing reactive oxygen species (ROS) to induce cell death.[18] Moreover, their ultrasmall size facilitates the penetration of microbial cell walls, resulting in better permeability than conventional antibacterial materials.[19] Numerous studies have confirmed the appreciable antimicrobial and antibiofilm activities of Au NPs modified with plant-derived compounds such as terpenoids,[20] flavonoids,[21,22] and phenols.[23]

Daidzein, known as 4′,7-dihydroxyisoflavone, is a natural phytoestrogenic isoflavone present in leguminous plants such as soybean and mungbean. This compound has received widespread attention owing to its antitumor, anti-inflammatory, antioxidant, and neuroprotective properties.[24] Studies have established that daidzein functions as a phytoestrogen and possesses anticancer mechanisms. For example, it prevents breast cancer via estrogen receptor modulation and its antiangiogenic properties. In addition, it suppresses ovarian cancer metastasis by regulating the PI3K/Akt signaling pathway.[25,26] Given its intrinsic antioxidant properties, daidzein exhibits multimodal therapeutic potential for oxidative stress-related disorders, especially in alleviating aging-related degeneration and preventing cardiovascular diseases.[27] The neuroprotective action of daidzein is achieved via receptor interactions (ERβ and GPR30) or PPARγ pathway activation, mitigating cellular toxicity in neuronal populations.[28] The pleiotropic pharmacological profile of daidzein renders it a highly promising candidate for drug development. In addition, the flavonoid has two hydroxyl groups and demonstrates reducing properties. The -OH group of flavonoids has been reported to reduce metal ions to Au NPs.[29] Flavonoids not only help reduce metal ions to nanosize but also play a role in the capping of Au NPs, facilitating their stability and biocompatibility.[30] Although daidzein has the potential to synthesize Au NPs, no studies have explored the in vivo and in vitro antimicrobial effects of Daidzein_Au NPs on CRE. Therefore, this research examined the antimicrobial effects and potential mechanisms of Daidzein_Au NPs, which may provide a new reference strategy for antimicrobial therapy.

Methods

Strains

The 15 clinical isolates of CRE used in this experiment were obtained from the First Affiliated Hospital of Wenzhou Medical University, which included five strains each of *Klebsiella pneumoniae, Escherichia coli*, and *Enterobacter cloacae*; these strains were identified by matrix-assisted laser desorption/ionization time-of-flight mass spectrometry (bioMérieux, Lyons, France). *Klebsiella pneumoniae* ATCC 700603 was used for quality control of antimicrobial susceptibility testing. The strains were defined as "FKXXX" for *Klebsiella pneumoniae*, "DCXXX" for *Escherichia coli* and "CGXXX" for *Enterobacter cloacae*, where "XXXX" represents the unique laboratory identification number. All strains were cultured in Luria Bertani (LB) broth, stored at −80°C, and resuscitated from cryopreserved tubes on blood plates or LB agar plates before each experiment. Ethical review and approval were received from the Ethics Committee in Clinical Research of the First Affiliated Hospital of Wenzhou Medicine University (KY2025-R026). Owing to the retrospective nature of this study, informed consent was waived.

Preparation of Drugs

MEM, IMP, and ertapenem (ERT) were purchased from Wenzhou Kangtai Biotechnology and dissolved in sterile ultrapure water before use. Daidzein was purchased from MACKLIN and dissolved in dimethyl sulfoxide (DMSO). The final concentration of DMSO was <1% (v/v).

Green Synthesis

The preparation of Daidzein_Au NPs and Au NPs was performed using the one-pot method.[31,32] Briefly, daidzein (0.05 mmoL), Tween 80 (30 mg), and triethylamine (50 μL) were dissolved in 10 mL of water and sonicated for 5 min. The mixture was stirred at 1000 rpm for 15 min, after which 500 μL of $HAuCl_4$ (0.05 mmoL) was added and the mixture

was stirred continuously for 2 h. The solution turned blue-purple, and Daidzein_Au NPs were formed. Furthermore, the sodium citrate reduction method prepared Au NPs without any modification. Daidzein_Au NPs and Au NPs were dialyzed in double-distilled water for 24 h and filtered through a 0.22-μm filter to remove bacteria.

Characterization

A multifunctional enzyme labeler was used to measure the ultraviolet-visible spectroscopy (UV-vis) absorption of the Daidzein_AuNPs. The crystal structure of Daidzein_Au NPs was analyzed by using an X-ray diffractometer (XRD). The morphology of gold nanoparticles was characterized by transmission electron microscopy (TEM). The functional groups of Daidzein_Au NPs were characterized by Fourier-transformed infrared spectroscopy (FTIR). Nanoparticles charge and dispersion properties were assessed by applying a nanoparticles-size zeta-potential analyzer (Dynamic Light Scattering [DLS]).

Antimicrobial Susceptibility Testing

The minimum inhibitory concentrations (MICs) of MEM, IMP, ERT, daidzein, Au NPs, and Daidzein_Au NPs against the CRE strains (see Table 1) were determined by using the microdilution broth method described by the CLSI, 2023.[33] Briefly, each drug was configured with 4 times the desired concentration, and 100 μL of successive 2-fold dilution concentrations of the drug was added into the well of a 96-well microtitre plate. Then, the bacterial suspensions were diluted to 10^6 CFU/mL, and 100 μL was added to each well. The MIC value was defined as the lowest concentration that could completely inhibit bacterial growth, as determined through the visual inspection after incubation for 16–20 h at 37°C, specifically, the absence of visible turbidity in the culture medium upon visual examination.[34]

Growth Curves and Time Kills

We selected FK9250, DC7114, and CG1038 to further evaluate the effect of Daidzein_Au NPs on CRE, and the strains were cultured in an LB medium with a starting inoculum of 10^6 CFU/mL. Four treatment groups were set up for each strain: a blank-control group (phosphate-buffer solution, PBS), a daidzein group (41.3 μg/mL based on the Daidzein_Au NPs concentration), Au NPs (32 μg/mL) group, and Daidzein_Au NPs (32 μg/mL) group. The samples were incubated at 37°C, 180 rpm with

Table 1 Drug Resistance and Mechanism of Clinical Strains (MIC, μg/mL)

Species	Strain	Antimicrobial Mechanism	MEM	IMP	ERT
Klebsiella pneumoniae	FK2836	KPC-2, IMP	64	128	256
	FK3006	KPC-2, IMP	128	32	256
	FK7112	KPC-2, OmpK37mutation	128	64	512
	FK7513	NDM-5	64	32	128
	FK9250	NDM-5	128	128	64
Escherichia coli	DC5113	KPC-2, TEM, CTX-M-1, CTX-M-9	16	8	128
	DC5293	TEM, SHV	64	0.25	128
	DC7114	TEM, SHV	32	16	128
	DC7706	TEM, SHV	64	32	256
	DC8647	NDM-1	32	16	128
Enterobacter cloacae	CG1038	KPC-2, AmpC	32	8	128
	CG1181	SHV, TEM, CTX-M-1, CTX-M-9, CTX-M-14	<0.25	2	128
	CG1257	IMP	4	32	64
	CG1330	NDM-1	8	16	128
	CG1381	OXA-23	32	32	64
Klebsiella pneumoniae	ATCC700603	/	0.25	0.25	0.5

Notes: The antibacterial mechanism was referred to previous studies.[35] Strains were defined as "FKXXX" for *Klebsiella pneumoniae*, "DCXXX" for *Escherichia coli* and "CGXXX" for *Enterobacter cloacae*, where "XXXX" represents the unique laboratory identification number.

Abbreviations: MEM, meropenem; IMP, imipenem; ERT, ertapenem; KPC, *Klebsiella pneumoniae* carbapenemase; NDM, New Delhi metallo-β-lactamase; TEM, Temoniera; CTX, Cefotaximase; SHV, Sulfhydryl variable; OXA, Oxacillinase.

shaking, and at predetermined time points (0, 2, 4, 6, 12, and 24 h), 200 μL was removed from each treatment mixture, and the absorbance was measured at 600 nm. Meanwhile, 100 μL of the culture fluid was removed at each time point for 10-fold gradient dilution, and 10 μL of the fluid was aspirated from the appropriate dilutions and incubated on LB agar plates for enumeration of the bacterial colonies (CFU/mL); each experiment was repeated thrice. A bactericidal effect was defined as a decrease by ≥ $3\log_{10}$ CFU/mL when compared with the control groups.[36,37]

Scanning Electron Microscopy (SEM)

To observe the effect of Daidzein_Au NPs on the morphology of bacteria. FK9250 bacterial suspension (approximately 1×10^8 CFU/mL) was treated with Daidzein_Au NPs (32 μg/mL) for 2 and 4 h, respectively. The drug-free treatment group (PBS group) was used as a control and centrifuged at 6000 rpm for 5 min. The bacterial suspension was removed, dried, and fixed for 2 h with 2.5% v/v glutaraldehyde. The samples were then treated with a gradient series of ethanol for 10 min and then dropped on silicon wafers (soaked in 75% ethanol overnight) to be subsequently gold-plated for observation under SEM.

Inner and Outer Membrane Permeability

Based on the morphological changes of SEM, the damage of Daidzein_Au NPs on the inner and outer membranes of bacteria was further verified. Bacteria were cultured overnight in LB broth, adjusted to an OD_{600} of 0.3–0.4 after washing twice with PBS; a total of 900 μL of the bacterial solution and 100 μL of the drug (drug concentration designed as 8 μg/mL and 16 μg/mL) were added to each treatment group without adding any drug as a blank control and treated with shaking for 2 or 2.5 h. Centrifugation was performed at 4,000 rpm, 5 min and then washed with PBS twice, after which 1 mL of the prepared N-phenyl-1-naphthylamine (NPN) solution (30 μM) or 1 mL of propidium iodide (PI) solution (50 μg/mL) were added and the solution was incubated at 37°C for 0.5 h.[38] The fluorescence intensity was measured by using an enzyme marker at an excitation/emission wavelength of NPN of 350 nm/420 nm to determine the permeability of outer membranes, with the excitation/emission wavelength set to 535 nm/615 nm to determine the permeability of the inner membrane by using the PI. The experiment was repeated thrice.

Reactive Oxygen Species (ROS) Assay

In order to determine the effect of the Daidzein_Au NPs on the levels of ROS in bacteria, we used a commercial kit (Beyotime, Beijing, China) to test the ROS generation.[39,40] Briefly, bacterial suspensions (OD_{600} 0.3–0.4) were incubated with 10 μM of dichlorodihy drofluorescein diacetate (DCFH-DA) probe for 45 min, and the cells were washed twice with PBS to remove the free probe. The cells were then resuspended in the same volume of PBS and treated with the daidzein (20.6 μg/mL and 41.3 μg/mL), Au NPs (16 μg/mL and 32 μg/mL), and Daidzein_Au NPs (16 μg/mL and 32 μg/mL) for 2 h at 37°C. PBS was used as a control. The fluorescence intensity was measured by using a microplate reader (Bio Tek, Synergy NEO2) at excitation/emission wavelengths of 488 and 535 nm.

Red Blood Cell Hemolysis Test and CCK8 Assay

Briefly, 5% of the RBC suspension was prepared by obtaining fresh blood from healthy mice, incubated with different concentrations of Daidzein_Au NPs (1–64 μg/mL) for 2 h at 37°C, and centrifuged at 3000 rpm for 5 min, after which the OD_{450nm} was determined. PBS was used as a negative control, and the positive control contained 0.1% Triton X-100. A hemolysis rate of <5% was considered to be safe. To 100 μL (1×10^5 cells) of RAW 264.7 mice macrophages, human kidney-derived HK-2 cells or human HepG2 cells were added, and 10 μL of different concentrations of Daidzein_Au NPs (1–64 μg/mL) were added for 24 h to each well. After incubation, 10 μL of the Cell Counting Kit-8 (CCK-8) reagent (Solarbio, China) was added to each well. The cells were then incubated for 1 h at room temperature, away from light, and the OD_{450nm} was measured. The cell viability was calculated using the following formula:

$$\text{Cell viability}\,(\%) = (\text{absorbance of sample} - \text{absorbance of medium})/(\text{absorbance of negative control} - \text{absorbance of medium}) \times 100.$$

Abdominal Infection Model

We established a mice model of acute abdominal infection to assess the therapeutic efficacy of Daidzein_Au NPs using specific-pathogen-free (SPF) grade male ICR mice (age: 6–8 weeks). Ethical review and approval were obtained from the Ethics

Committee of the First Affiliated Hospital of Wenzhou Medical University (Approval No.: SYXK 2021-0017). In the text animals, a bacterial suspension (100 μL, 2×10^8 CFU/mL) supplemented with 5% yeast extract was injected into the abdominal cavity to create an infection, followed by drug administration 2 h later.[23] PBS was used as a control, and 2.5 mg/kg colistin served as the positive control. The remaining daidzein, Au NPs, Daidzein_Au NPs three groups of animals were injected intraperitoneally with 2.5 mg/kg of different drugs and monitored to observe the 3-day survival rate, followed by colony counting in peritoneal lavage fluid to assess the treatment efficacy.

Bioinformatics Analysis

The total RNA of FK9250 from the blank-control group and the Daidzein_Au NPs treatment group (3 biological replicates for each group) was extracted with trizol (Invitrogen, USA) as per the instructions. After quality control and mRNA enrichment, the cDNA was synthesized using RNA as a template for subsequent RNA-seq library preparation. Next-generation sequencing was performed to sequence the ends of the library based on the Illumina sequencing platform.[41]

Differentially expressed genes (DEGs) were identified using a transcriptome analysis console (fold change > 1.5, $P < 0.05$). Kyoto Encyclopedia of Genes and Genomes (KEGG) and Gene Ontology (GO)[42] were performed using KOBAS and DAVID. KEGG (Kanehisa et al 2008) is a database resource for interpreting high-level functions and utilities in biological systems (http://www.genome.jp/keg/).

Statistical Analysis

The figures were drawn using GraphPad Prism 8, and the data in the graphs are presented as the mean and standard deviation. Unpaired *t*-test was performed for comparing between two groups, and one-way ANOVA and Tukey's multiple comparison test were performed for comparing multiple groups, while the survival curves were constructed by using the Kaplan–Meier method. Statistical significance was set at $P < 0.05$.

Results

Au NP Synthesis and Characterization

Daidzein possesses two reducing hydroxyl groups and has the potential to synthesize Au NPs. In this study, Au NPs and Daidzein_Au NPs were synthesized using a one-pot method. UV absorption spectra revealed that the absorption peak of Daidzein_Au NPs was at 533 nm (Figure 1A). The results of the XRD analysis of Daidzein_Au NPs were presented in Figure 1B. Based on the diffraction pattern, the characteristic peaks at 2θ values of 38.1° (111), 44.3° (200), 64.6° (220), and 77.7° (311) were consistent with the face-centered cubic gold planes reported in the literature (JCPDS file no: 04–0784).[43] The sharp XRD peaks indicate excellent crystallinity, and no impurity peaks are observed, confirming the high purity of Daidzein_Au NPs, a high crystallinity of 79% is achieved. In addition, TEM images (Figure 1C) indicated that Daidzein_Au NPs exhibited a spherical morphology, showing good monodispersity and uniform size distribution. Which indicates that the successful production of Daidzein_Au NPs.

FTIR analysis further validated the successful synthesis of Daidzein_Au NPs. As depicted in Figure 1D, daidzein was replete with polar groups and possessed a conjugated aromatic ring system characterized by high electron density. The absorption peak at 3200 cm^{-1} could be attributed to the O-H stretching vibration mode derived from the phenolic hydroxyl structure. Meanwhile, the absorption peak at 1633 cm^{-1} could be primarily associated with the stretching vibration mode of the ketone carbonyl C=O. When examining the infrared spectra of Daidzein_Au NPs, the absorption peak shift at 3080 cm^{-1} suggested that the phenolic hydroxyl group of daidzein was adsorbed and crosslinked to the Au surface via coordination or hydrogen bonds. The stretching vibration peak of C=O, originally around 1735 cm^{-1}, shifted to 1686 cm^{-1}. This shift indicated that the carbonyl group donates lone pairs of electrons and engages in weak coordination with the gold surface. The absorption peaks near 1261 cm^{-1} and 1098 cm^{-1} could be ascribed to the bending vibration of daidzein C-OH and the stretching vibration mode of C-O in Au NPs, respectively. The presence of these absorption peaks asserted that daidzein undergoes coordination adsorption and hydrogen bonding with the surface of Au NPs via its phenolic hydroxyl and carbonyl groups, forming stable complexes.

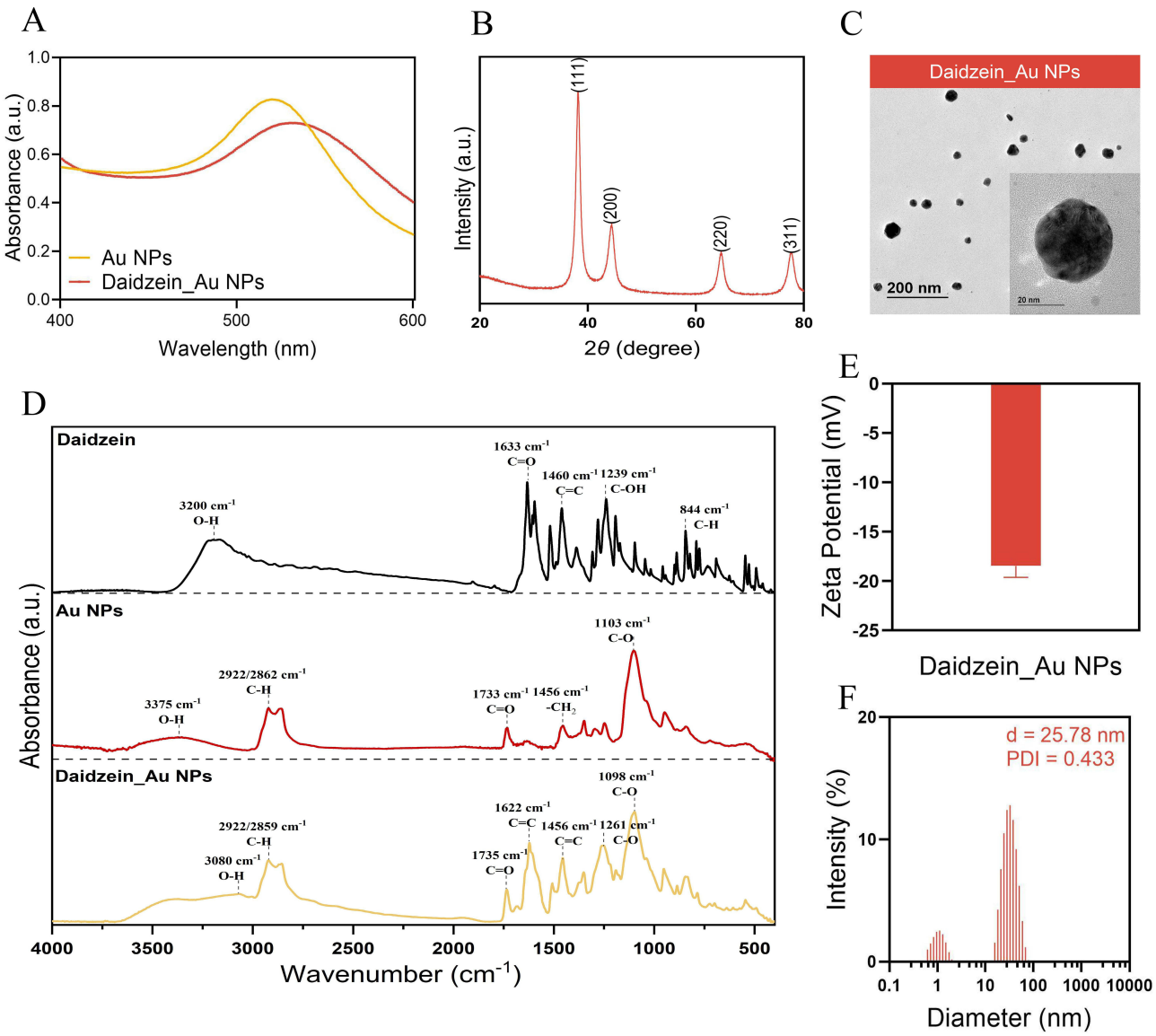

Figure 1 Characterizations of Daidzein_Au NPs. (**A**) Ultraviolet absorption spectrum of Daidzein_Au NPs; (**B**) The XRD pattern of Daidzein_Au NPs; (**C**) TEM image of Daidzein_Au NPs; (**D**) FTIR spectra of Daidzein_Au NPs, daidzein, and Au NPs. (**E**) Characterization of the Zeta potential of Daidzein_Au NPs; (**F**) Particle size of Daidzein_Au NPs, as analyzed by DLS.

In addition, the structure was characterized using DLS, which demonstrated that the average particle size was 25.78 nm and that the polydispersity index was 0.433, implying that the particles were small in size and relatively uniformly dispersed. The average zeta-potential value was −18.5 mV with a negative charge (Figure 1E and F), providing stability.

Determination of MIC

To test their antimicrobial effects, 15 CRE strains (Table 1) whose MICs are known to be 8–256 μg/mL were included. The main types of resistance genes were those encoding Ambler class A, such as KPC, TEM, SHV, and CTX-M type. In addition, other resistance mechanisms, such as NDM, IMP, AmpC, and OXA-23, were identified. The antimicrobial effects of Daidzein_Au NPs against CRE strains were further investigated (see Table 2). Daidzein and Au NPs showed poor antimicrobial effects against these CRE strains with drug sensitivity >256 μg/mL, whereas Daidzein_Au NPs showed good antimicrobial effects with an 8–16 μg/mL MIC.

https://doi.org/10.2147/IJN.S515798

Table 2 Drug Sensitivity of Daidzein_Au NPs to CRE Strains (MIC, μg/mL)

Species	Strain	Daidzein	Au NPs	Daidzein_Au NPs
Klebsiella pneumoniae	FK2836	≥256	≥256	16
	FK3006	≥256	≥256	16
	FK7112	≥256	≥256	16
	FK7513	≥256	≥256	16
	FK9250	≥256	≥256	16
Escherichia coli	DC5113	≥256	≥256	8
	DC5293	≥256	≥256	16
	DC7114	≥256	≥256	16
	DC7706	≥256	≥256	16
	DC8647	≥256	≥256	16
Enterobacter cloacae	CG1038	≥256	≥256	16
	CG1181	≥256	≥256	16
	CG1257	≥256	≥256	16
	CG1330	≥256	≥256	16
	CG1381	≥256	≥256	16

Notes: Strains were defined as "FKXXX" for *Klebsiella pneumoniae*, "DCXXX" for *Escherichia coli* and "CGXXX" for *Enterobacter cloacae*, where "XXXX" represents the unique laboratory identification number.

Verification of the Antibacterial Effect of Daidzein_Au NPs

One strain was selected from each type of bacterium. When using a concentration of 32 μg/mL, compared with the other three groups, bacterial growth was significantly inhibited in the Daidzein_Au NPs-treated groups of FK9250, DC7114, and CG1038 (Figure 2A). Colony counting showed that the bactericidal process started at 4 h, and the count decreased by at least 3 $\log_{10}$ CFU/mL at 24 h compared with the other three groups, signifying a good bactericidal effect (Figure 2B). SEM analysis of the bacterial cells to determine the morphological changes revealed that those in the PBS group were regular and rod-shaped, with an intact cell membrane. However, after treatment with Daidzein_Au NPs, FK9250 exhibited membrane rupture at 2 h, with more severe rupture at 4 h (Figure 3), proving the rapid bactericidal effect of the formulation.

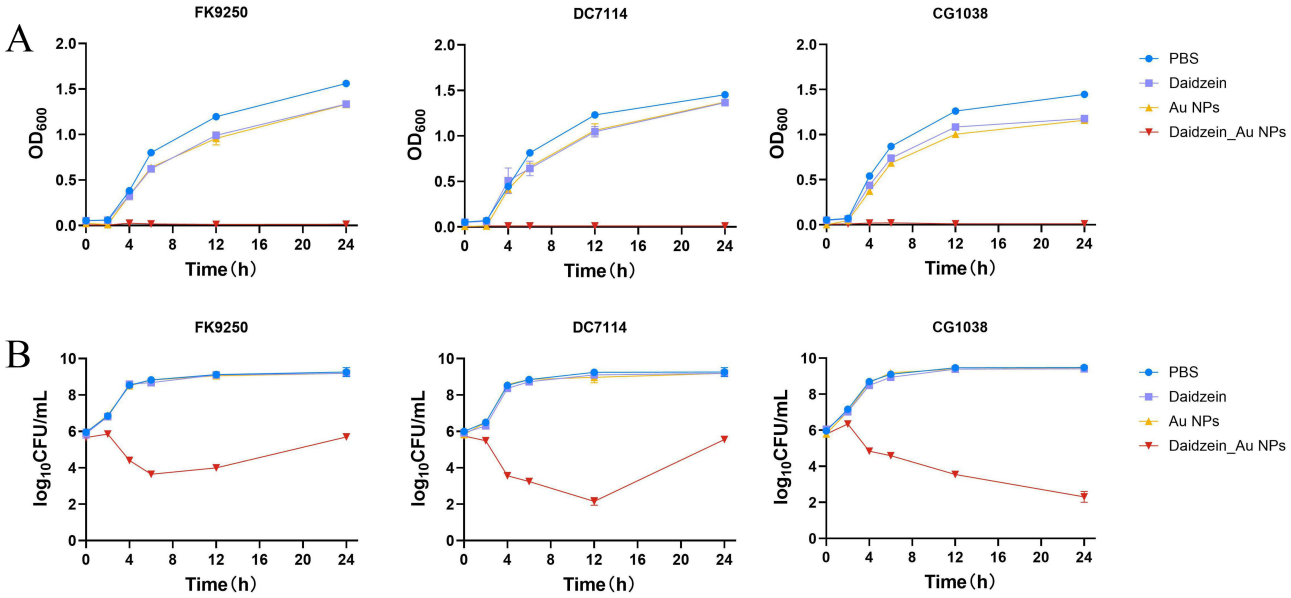

Figure 2 The antimicrobial ability of Daidzein_Au NPs in vitro. Growth curves (**A**) and time-kill curves (**B**) of clinical CRE strains after treatment with Daidzein_Au NPs (2 MIC).

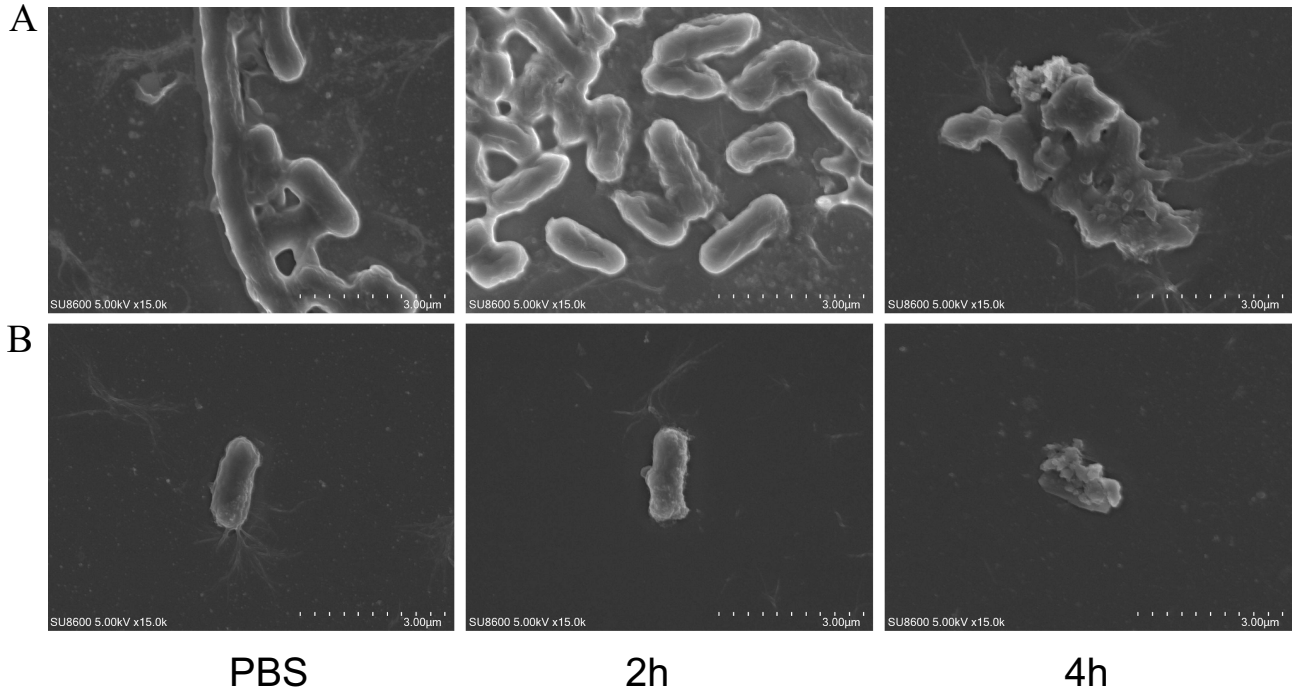

Figure 3 Morphological changes of FK9250 strain under SEM after 2 h or 4 h treatment with Daidzein_Au NPs (2 MIC) when compared with the PBS-treatment group. The morphology changes of FK9250 strain multiple bacteria (**A**) and single bacteria (**B**) were observed after 2 h or 4 h of treatment with Daidzein_Au NPs (2 MIC).

The Bactericidal Mechanism of Daidzein_Au NPs

To further explore the mechanism of bactericidal action of Daidzein_Au NPs based on the SEM results of cell membrane disruption, NPN and PI fluorescent dyes were applied to quantify the permeability of the bacterial outer and inner membranes and incubated for 1.5 h and 2 h, respectively. The findings showed that the fluorescence intensities of NPN and PI were higher in the Daidzein_Au NPs-treated groups of 1/2 MIC (8 μg/mL) and MIC (16 μg/mL) of FK9250, DC7114, and CG1038 than those in the PBS group (Figure 4A and B). These observations agreed with the SEM results. Subsequent ROS measurements of these three strains indicated that the elevation of ROS within the bacterial cells was increased in the Daidzein_Au NPs treatment group (Figure 4C).

The Biocompatibility of Daidzein_Au NPs

Before evaluating the in vivo bactericidal effect, biocompatibility assays for Daidzein_Au NPs were performed. The results of the hemolysis assay illustrated that hemolysis did not occur at Daidzein_Au NPs concentrations of ≤64 μg/mL (Figure 5A). Regarding the cytotoxicity assay (Figure 5B–D), RAW 264.7 mouse macrophages, human kidney-derived HK-2 cells, or human HepG2 cells were used for cytotoxicity experiments. The results confirmed that Daidzein_Au NPs did not exert cytotoxic effects on macrophages, hepatocytes, or kidney cells at the experimental concentration. Significant effects on cell viability were not noted in the concentration range used in the experiment. Overall, Daidzein_Au NPs were preliminarily found to be safe at sterilizing concentrations.

Antimicrobial Effect in vivo

The mouse model of acute abdominal infection was used for the in vivo assessment of antimicrobial efficacy, and 2×10^7 CFU FK9250 was administered to infected mice for 2 h. Subsequently, the corresponding therapy was initiated. Daidzein_Au NPs were administered at a concentration of 2.5 mg/kg, and the survival rate of the mice was monitored every 12 h. The PBS group served as the control group. As portrayed in Figure 6A, the 72 h survival rate of mice treated with Daidzein_Au NPs was 100%, the same as that of the positive control group (the Colistin group). In contrast, the survival rates of the PBS, daidzein, and Au NPs groups were only approximately 30% at 72 h, establishing that the survival rate of mice treated with Daidzein_Au NPs was

https://doi.org/10.2147/IJN.S515798

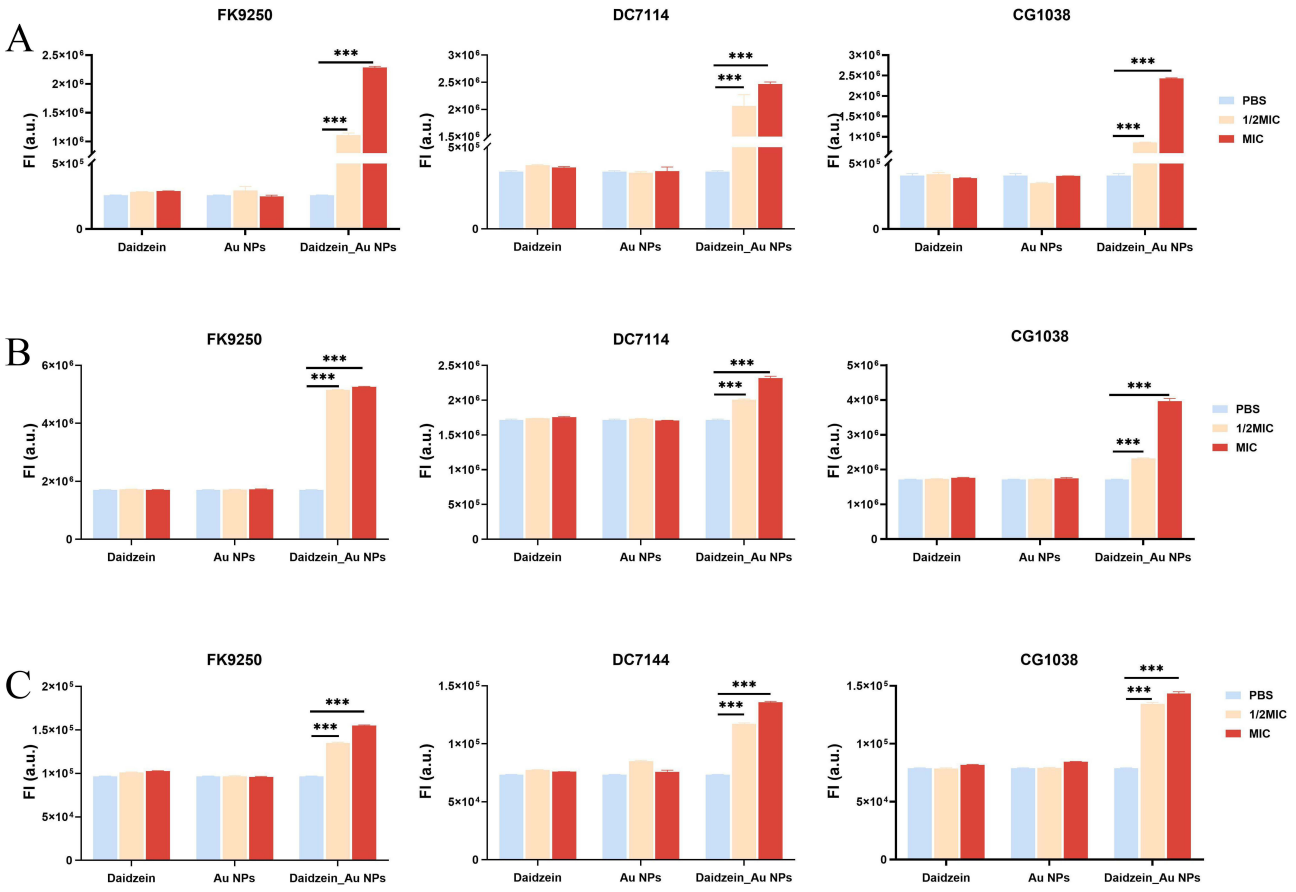

Figure 4 Changes in the membrane permeability and reactive oxygen species after treatment with Daidzein_Au NPs. The fluorescence intensity of NPN (**A**) and PI (**B**) after treatment with different drugs. (**C**) Fluorescence intensity analysis of intracellular ROS in CRE strains. ***$P < 0.001$.

significantly improved. In addition in the Daidzein_Au NPs-treated group, the colony counts in the intraperitoneal lavage were higher than those in the Colistin group (positive control) but significantly lower than those in the control, daidzein, and Au NPs groups (Figure 6B), confirming that Daidzein_Au NPs also exhibit a certain antibacterial activity potential in vivo.

RNA-Seq Results

Transcription analysis was performed for FK9250 in control and Daidzein_Au NPs-treated groups. Compared with the control group, a total of 187 transcripts were significantly differentially expressed in the Daidzein_Au NPs-treated group (|fold change| >1.5, $p < 0.05$), of which 125 were upregulated and 62 were downregulated (Figure 7A). These DEGs were subjected to GO enrichment analysis, and the GOs were classified into three main categories: biological processes (BPs), cellular components (CCs), and molecular functions (MFs). According to the results of GO analysis presented in Figure 7B, the methionine metabolic process, methionine biosynthetic process, phosphoenolpyruvate-dependent sugar phosphotransferase system, and carbohydrate import across the plasma membrane were the BPs intricately linked to the DEGs. Regarding CCs, the enriched subcategory was exodeoxyribonuclease VII complex. Finally, in MFs, 5-methyltetrahydropteroyltriglutamate-homocysteine S-methyltransferase activity, diamine N-acetyltransferase activity, D-glucosamine phosphotransferase system (PTS) permease activity, and carbohydrate-binding were the most enriched subcategories. Furthermore, metabolic pathways related to carbohydrate binding and transmembrane transport were enriched. The KEGG results suggested that the DEGs were associated with PTS; alanine, aspartate, and glutamate metabolism; arginine and proline metabolism; porphyrin metabolism; and valine, leucine, and isoleucine degradation pathway (Figure 7C). These pathways were associated with metabolic alterations. The heatmap (Figure 8) illustrated that most metabolism-related genes were downregulated, including *asnA, asnB, cbiH, puuA*, and *glaH*, whereas *glnA, speG, hemF*, etc., were upregulated.

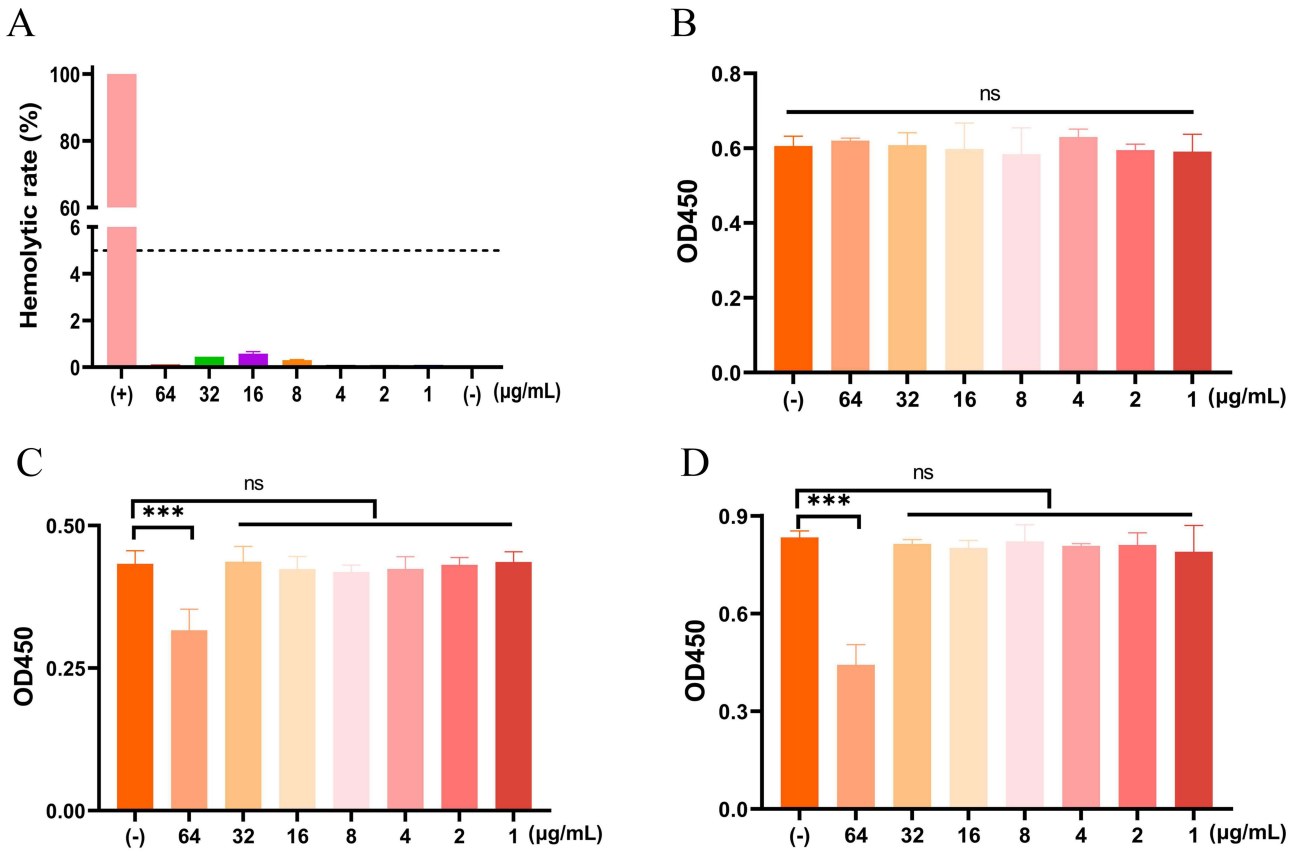

Figure 5 The Biocompatibility of Daidzein_Au NPs. (**A**) The hemolytic effects of Daidzein_Au NPs at different concentrations; (**B**) Safety assessment of different concentrations of Daidzein_Au NPs in macrophages; (**C**) Safety assessment of different concentrations of Daidzein_Au NPs in human kidney-derived HK-2 cells; (**D**) Safety assessment of different concentrations of Daidzein_Au NPs in human HepG2 cells. ***$P < 0.001$.
Abbreviation: ns, no significance.

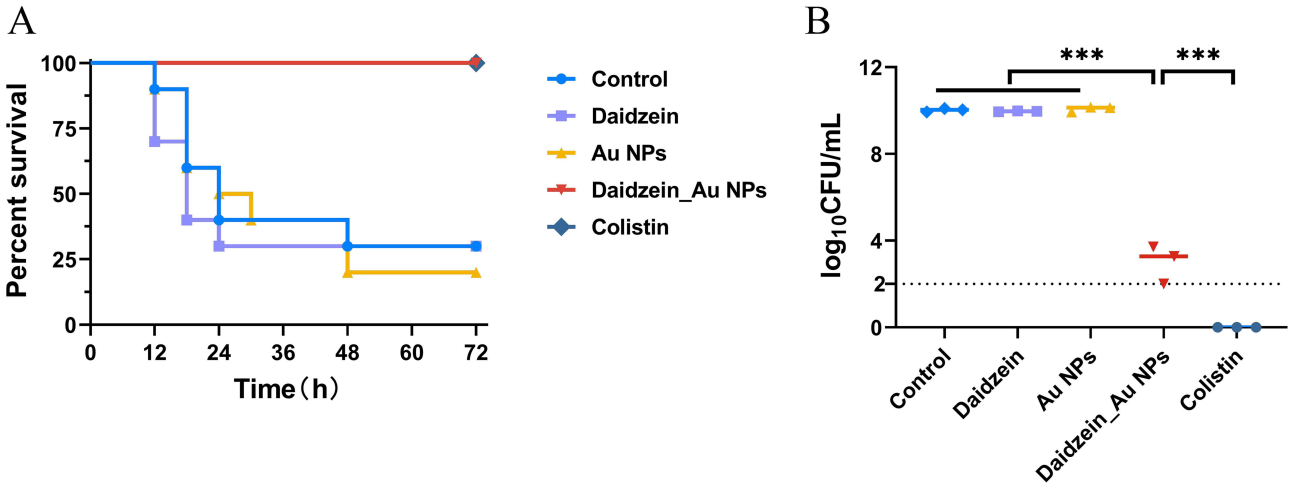

Figure 6 The therapeutic effect of Daidzein_Au NPs on mice with abdominal infection. (**A**) Survival of mice in different treatment groups; (**B**) Colony loading results of peritoneal lavage fluid in mice of different administration groups. The dotted line represents the minimum detection limit. ***$P < 0.001$.

https://doi.org/10.2147/IJN.S515798

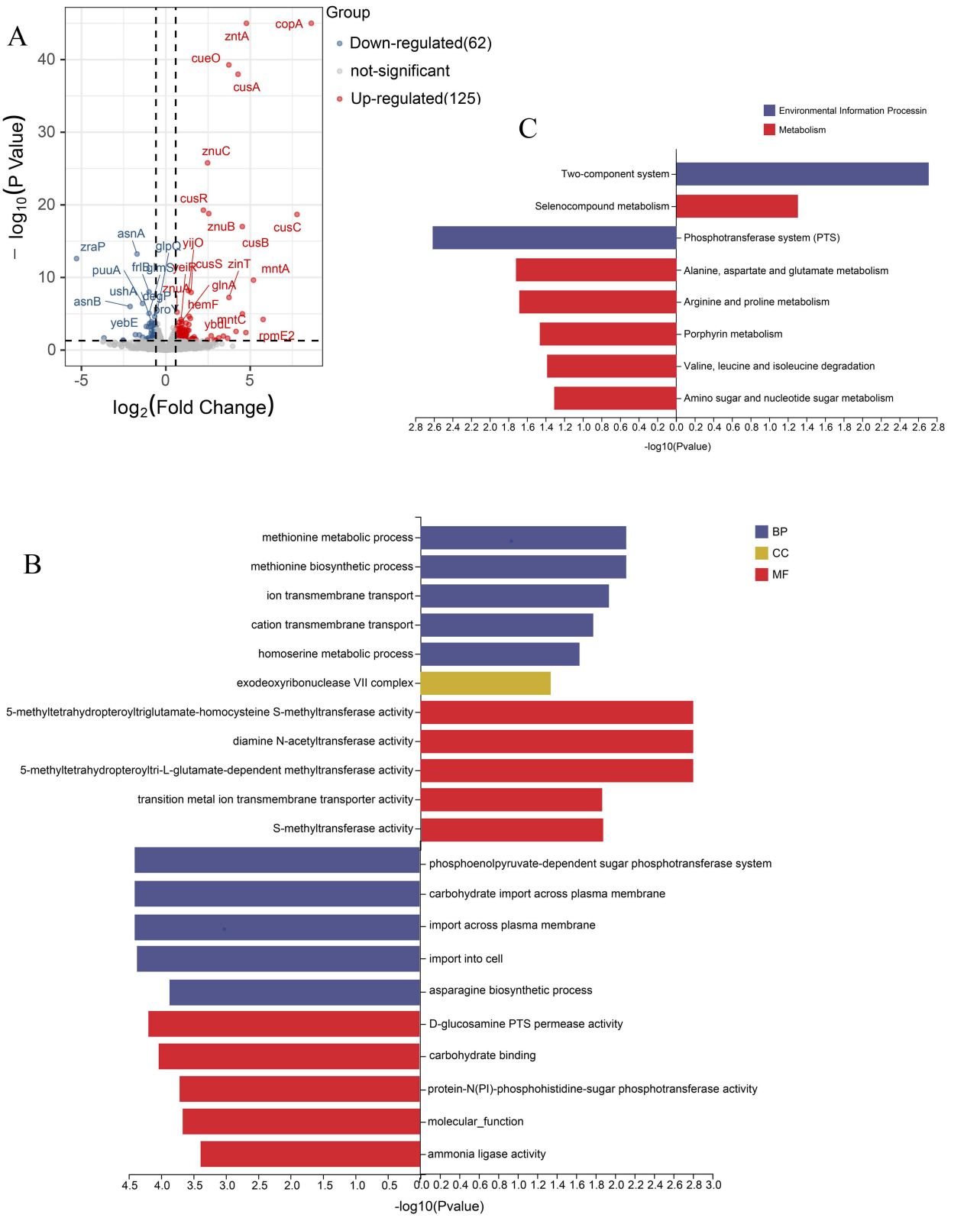

Figure 7 Bioinformatics analysis in Daidzein_Au NPs treatment and control FK9250 strains. (**A**) Visualization of volcano plots of DEGs; (**B**) GO enrichment analysis of DEGs. Right: up, left: down. (**C**) KEGG analysis of DEGs between Daidzein_Au NPs treated and control groups. Right: up, left: down.
Abbreviations: BP, biological process; CC, cellular component; MF, molecular function.

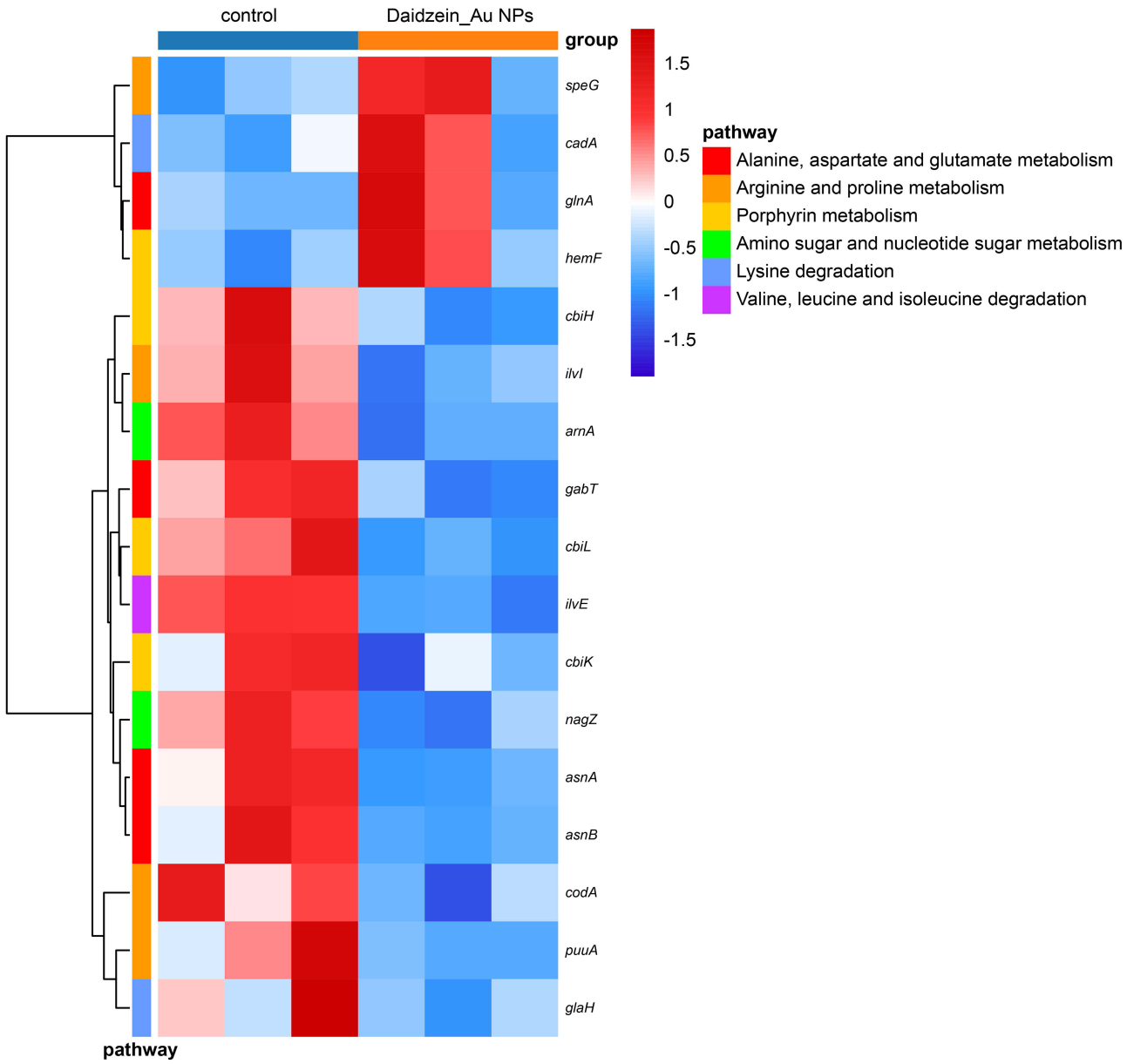

Figure 8 Heat map of some of the metabolism-related genes.

Discussion

Antibiotic resistance has become a global concern, and there is an urgent need to identify novel therapeutic strategies for CRE strains with limited options for antibiotic use. Nanogold, which is widely used in the medical industry because of its unique properties, exhibits multiple potential mechanisms for sterilization. In this study, Daidzein_Au NPs were synthesized by reducing Au^{3+} to Au^{0} using the plant compound daidzein as a reducing agent. In vitro and in vivo experiments verified the antimicrobial effect and biosafety of the Daidzein_Au NPs, paving the way for their application in antimicrobial therapy.

The size and shape of Au NPs considerably affect their antimicrobial activity. Spherical particles have high absorption efficiency; the smaller the particle size, the stronger the antimicrobial effect.[44] Characterization studies revealed that Daidzein_Au NPs were successfully synthesized and that they displayed a small particle size (25.78 nm) and a round-like shape. The MIC of Daidzein_Au NPs against the tested CRE strains was 8–16 μg/mL. Both growth curves and time–kill

https://doi.org/10.2147/IJN.S515798

experiments confirmed their antimicrobial activity. Colony counting showed that the bactericidal process started at 4 h, and the count decreased by at least 3 $\log_{10}$ CFU/mL at 24 h compared with the control, daidzein, and Au NPs groups. To ensure safety and biocompatibility, hemolysis and CCK8 assays were performed, and the results indicated that Daidzein_Au NPs were preliminarily safe at sterilizing concentrations. In addition, an acute abdominal infection mouse model was established for in vivo experiments, which revealed that the survival rate of the Daidzein_Au NPs treatment group was significantly increased and the colony load of abdominal infection was reduced. Based on these observations, Daidzein_Au NPs are expected to become a novel and promising antimicrobial material.

Antibiotics used in the clinic have specific targets, and the antibacterial mechanism can be divided into five categories according to the biological function of their target: inhibition of cell wall, protein, and nucleic acid synthesis; depolarization of the cell membrane; and inhibition of metabolic pathways.[45] Nanomaterials have a smaller diameter than conventional antibiotics and their size is significantly different, accounting for the differences in their bactericidal mechanisms. The currently known antibacterial mechanisms of nanomaterials include membrane disruption, electron transport chain disruption, catalytic killing, inhibition of protein and DNA synthesis, and dysregulation of bacterial metabolism.[44,46] Of these, membrane disruption is one of the key antimicrobial mechanisms of nanomaterials. In this study, SEM showed that after treating FK9250 with Daidzein_Au NPs for 2–4 h, the bacterium underwent obvious disruption of cell membranes. In addition, quantitative determination of inner and outer membrane permeability revealed that the permeability of the Daidzein_Au NPs-treated group was significantly higher than that of the other three groups, which aligns with the SEM findings. This observation confirmed that membrane disruption is one of the antimicrobial mechanisms of Daidzein_Au NPs. Redox reactions are involved in various biological processes in microorganisms[47] and are one of the main pathways for ROS production. The entry of Au NPs into the microbial cell and interference with the propagation of the electron transport chain can enhance ROS production.[48] ROS induces cellular oxidative stress, leading to cell death. In this study, 1/2 MIC and MIC concentrations of Daidzein_Au NPs caused a significant increase in ROS within the bacteria, asserting that the increase in ROS production is one of the antimicrobial effects of Daidzein_Au NPs.

In addition, cellular metabolism has a profound impact on bacterial growth. Transcriptomic studies demonstrated that Daidzein_Au NPs downregulated several metabolic pathways in bacteria. Alanine, aspartate, and glutamate metabolism; arginine and proline metabolism; and amino sugar and nucleotide sugar metabolic pathways were closely linked to energy metabolism. Furthermore, *glaH* expression was significantly downregulated, and in KEGG enrichment analysis, this gene was involved in regulating the conversion of glutaraldehyde to succinate. The latter is a crucial intermediate in the tricarboxylic acid cycle and may reduce energy synthesis,[49] affecting bacterial growth and reproduction. Moreover, studies have confirmed that altering the metabolic state of bacteria is beneficial in countering drug resistance.[50,51] Exogenous metabolites can reprogram the bacterial metabolome from a drug-resistant to a drug-sensitive phenotype.[52,53] Huang et al found that L-glutamine could act synergistically with rifampicin against persistent mycobacteria.[54] Moreover, L-glutamine has been documented to augment the antibacterial effect of gentamicin against resistant *E. coli* and methicillin-resistant *Staphylococcus aureus*.[55,56] This study found that *glnA* was significantly upregulated, which may increase glutamine synthesis and enhance the antibacterial effect of Daidzein_Au NPs as an adjuvant. In summary, Daidzein_Au NPs can effectively destroy cell membranes, accentuate ROS production, and alter the metabolic state of bacteria, exhibiting the potential to be applied clinically as antibacterial drugs.

Conclusion

Exploring nanomaterials with potential bactericidal effects can aid in combating the serious threat posed by rapidly evolving CRE strains. In this study, Daidzein_Au NPs were successfully synthesized. Systematic in vitro experiments and animal model studies established their significant antibacterial efficacy against CRE. Mechanistic investigations elucidated that this nanomaterial exerts its antibacterial effects via multiple pathways, including disruption of bacterial cell membrane integrity, induction of ROS generation, and interference with bacterial metabolic homeostasis. Safety evaluation revealed the absence of significant biotoxicity at effective antibacterial concentrations. Thus, Daidzein_Au NPs broaden the biomedical applications of daidzein and serve as a promising novel nano-antibacterial agent with translational potential for the clinical treatment of CRE infections. Their multi-mechanistic synergistic action offers new avenues to develop therapies for bacterial infections caused by CRE strains.

Abbreviations

Daidzein_Au NPs, daidzein-decorated gold nanoparticles; CRE, carbapenem resistant Enterobacteriaceae; NPN, N-phenyl-1-naphthylamine; PI, Propidium iodide; ROS, Reactive oxygen species; MIC, Minimum inhibitory concentration; MDR, multidrug-resistant; XDR, extensively drug-resistant; Au NPs, gold nanoparticles; LB, Luria Bertani; DMSO, dimethyl sulfoxide; DLS, dynamic light scattering; TEM, transmission electron microscopy; MEM, meropenem; IMP, imipenem; ERT, ertapenem; PBS, phosphate buffer solution; NGS, Next-Generation Sequencing; DEGs, Differentially expressed genes; PDI, polydispersity index; GO, Gene Ontology; KEGG, Kyoto Encyclopedia of Genes and Genomes.

Data Sharing Statement

The data used and analyzed in this study are included in this article and are available from the first author upon reasonable request.

Ethics Approval and Consent to Participate

Permission for using the raw data and the isolates for research purposes was approved by the Ethics Committee in Clinical Research of the First Affiliated Hospital of Wenzhou Medicine University (KY2025-R026). This retrospective study was conducted in accordance with the Declaration of Helsinki and was approved by the Clinical Research of the First Affiliated Hospital of Wenzhou Medicine University Ethics Committee (Approval No.: KY2025-R026). The need for individual patient consent was waived by the Ethics Committee due to the following reasons: The study involved only anonymized analysis of existing medical records; The research posed no more than minimal risk to participants; Obtaining consent was impracticable given the retrospective design and large cohort size. All data were de-identified prior to analysis, with direct identifiers (names, IDs) removed and indirect identifiers (dates, rare diagnoses) aggregated to prevent re-identification. Access to raw data was limited to authorized investigators under institutional data protection protocols.

The mice experiments were approved by the First Affiliated Hospital Ethics Committee of Wenzhou Medical University (Approval No. SYXK 2021–0017) and carried out in accordance with the Wenzhou Laboratory Animal Welfare and Ethics Guidelines.

Author Contributions

All authors made a significant contribution to the work reported, whether that is in the conception, study design, execution, acquisition of data, analysis and interpretation, or in all these areas; took part in drafting, revising or critically reviewing the article; gave final approval of the version to be published; have agreed on the journal to which the article has been submitted; and agree to be accountable for all aspects of the work.

Funding

This work was funded by Key Laboratory of Clinical Laboratory Diagnosis and Translational Research of Zhejiang Province (2022E10022).

Disclosure

The authors have no conflicts of interest to declare in this work.

References

1. Romandini A, Pani A, Schenardi PA, Pattarino GAC, De Giacomo C, Scaglione F. Antibiotic resistance in pediatric infections: global emerging threats, predicting the near future. *Antibiotics*. 2021;10(4):393. doi:10.3390/antibiotics10040393
2. Rodríguez-Baño J, Gutiérrez-Gutiérrez B, Machuca I, Pascual A. Treatment of infections caused by Extended-Spectrum-Beta-Lactamase-, AmpC-, and carbapenemase-producing Enterobacteriaceae. *Clin Microbiol Rev*. 2018;31(2):10–128. doi:10.1128/CMR.00079-17
3. Potter RF, D'Souza AW, Dantas G. The rapid spread of carbapenem-resistant Enterobacteriaceae. *Drug Resist Updat*. 2016;29:30–46. doi:10.1016/j.drup.2016.09.002

4. Slama TG. Clinical review: balancing the therapeutic, safety, and economic issues underlying effective antipseudomonal carbapenem use. *Crit Care*. 2008;12(5):233. doi:10.1186/cc6994
5. Tacconelli E, Carrara E, Savoldi A, et al. Discovery, research, and development of new antibiotics: the WHO priority list of antibiotic-resistant bacteria and tuberculosis. *Lancet Infect Dis*. 2018;18(3):318–327. doi:10.1016/S1473-3099(17)30753-3
6. Tsilipounidaki K, Athanasakopoulou Z, Müller E, et al. Plethora of resistance genes in carbapenem-resistant gram-negative bacteria in Greece: no end to a continuous genetic evolution. *Microorganisms*. 2022;10(1):159. doi:10.3390/microorganisms10010159
7. Kazmierczak KM, Rabine S, Hackel M, et al. Multiyear, multinational survey of the incidence and global distribution of metallo-β-lactamase-producing Enterobacteriaceae and pseudomonas aeruginosa. *Antimicrob Agents Chemother*. 2016;60(2):1067–1078. doi:10.1128/AAC.02379-15
8. Harding-Crooks R, Smith D, Fanning S, Fox EM. Dissemination of carbapenemase-producing Enterobacteriaceae and associated resistance determinants through global food systems. *Compr Rev Food Sci Food Saf*. 2023;22(4):2706–2727. doi:10.1111/1541-4337.13159
9. Li X, Ye H. Clinical and mortality risk factors in bloodstream infections with carbapenem-resistant Enterobacteriaceae. *Can J Infect Dis Med Microbiol*. 2017;2017:6212910. doi:10.1155/2017/6212910
10. Hu F, Guo Y, Zhu D, et al. CHINET surveillance of bacterial resistance: results of 2020. *Chin J Infect Chemother*. 2021;21(04):377–387. doi:10.16718/j.1009-7708.2021.04.001
11. Ramalingam V. Multifunctionality of gold nanoparticles: plausible and convincing properties. *Adv Colloid Interface Sci*. 2019;271:101989. doi:10.1016/j.cis.2019.101989
12. Khan T, Ullah N, Khan MA, Mashwani Z-U-R, Nadhman A. Plant-based gold nanoparticles: a comprehensive review of the decade-long research on synthesis, mechanistic aspects and diverse applications. *Adv Colloid Interface Sci*. 2019;272:102017. doi:10.1016/j.cis.2019.102017
13. Okamoto T, Nakamura T, Sakota K, Yatsuhashi T. Synthesis of single-nanometer-sized gold nanoparticles in liquid-liquid dispersion system by femtosecond laser irradiation. *Langmuir*. 2019;35(37):12123–12129. doi:10.1021/acs.langmuir.9b01854
14. Mikhailova EO. Gold nanoparticles: biosynthesis and potential of biomedical application. *J Funct Biomater*. 2021;12(4):70. doi:10.3390/jfb12040070
15. Gu X, Xu Z, Gu L, et al. Preparation and antibacterial properties of gold nanoparticles: a review. *Environ Chem Lett*. 2020;19(1):167–187. doi:10.1007/s10311-020-01071-0
16. Hong R, Han G, Fernández JM, Kim B-J, Forbes NS, Rotello VM. Glutathione-mediated delivery and release using monolayer protected nanoparticle carriers. *J Am Chem Soc*. 2006;128(4):1078–1079.
17. Nie H, Huang R, Jiang G, et al. Modulating active targeting nanoparticle design according to tumor progressions. *Acta Pharm Sin B*. 2025;15(2):1143–1158. doi:10.1016/j.apsb.2024.12.016
18. Lou-Franco J, Das B, Elliott C, Cao C. Gold nanozymes: from concept to biomedical applications. *Nanomicro Lett*. 2020;13(1):10. doi:10.1007/s40820-020-00532-z
19. Cai R, Cheng Q, Zhao J, et al. Sericin-assisted green synthesis of gold nanoparticles as broad-spectrum antimicrobial and biofilm-disrupting agents for therapy of bacterial infection. *Int J Nanomed*. 2025;20:3559–3574. doi:10.2147/IJN.S494616
20. Singh P, Pandit S, Garnæs J, et al. Green synthesis of gold and silver nanoparticles from Cannabis sativa (industrial hemp) and their capacity for biofilm inhibition. *Int J Nanomed*. 2018;13:3571–3591. doi:10.2147/IJN.S157958
21. Vijaya Kumar P, Mary Jelastin Kala S, Prakash KS. Green synthesis of gold nanoparticles using Croton Caudatus Geisel leaf extract and their biological studies. *Mater Lett*. 2019;236:19–22. doi:10.1016/j.matlet.2018.10.025
22. Rajan A, Vilas V, Philip D. Studies on catalytic, antioxidant, antibacterial and anticancer activities of biogenic gold nanoparticles. *J Mol Liq*. 2015;212:331–339. doi:10.1016/j.molliq.2015.09.013
23. Huang Z, Zhang X, Yao Z, et al. Thymol-decorated gold nanoparticles for curing clinical infections caused by bacteria resistant to last-resort antibiotics. *mSphere*. 2023;8(3):e0054922. doi:10.1128/msphere.00549-22
24. Singh S, Grewal S, Sharma N, et al. Unveiling the pharmacological and nanotechnological facets of Daidzein: present state-of-the-art and future perspectives. *Molecules*. 2023;28(4):1765. doi:10.3390/molecules28041765
25. Chan KKL, Siu MKY, Jiang Y-X, Wang -J-J, Leung THY, Ngan HYS. Estrogen receptor modulators genistein, daidzein and ERB-041 inhibit cell migration, invasion, proliferation and sphere formation via modulation of FAK and PI3K/AKT signaling in ovarian cancer. *Cancer Cell Int*. 2018;18:65. doi:10.1186/s12935-018-0559-2
26. Kaufman-Szymczyk A, Jalmuzna J, Lubecka-Gajewska K. Soy-derived isoflavones as chemo-preventive agents targeting multiple signalling pathways for cancer prevention and therapy. *Br J Pharmacol*. 2024;182(10):2259–2286. doi:10.1111/bph.16353
27. Goleij P, Sanaye PM, Alam W, et al. Unlocking daidzein's healing power: present applications and future possibilities in phytomedicine. *Phytomedicine*. 2024;134:155949. doi:10.1016/j.phymed.2024.155949
28. Kajta M, Rzemieniec J, Litwa E, et al. The key involvement of estrogen receptor β and G-protein-coupled receptor 30 in the neuroprotective action of daidzein. *Neuroscience*. 2013;238:345–360. doi:10.1016/j.neuroscience.2013.02.005
29. Dikshit PK, Kumar J, Das AK, et al. Green synthesis of metallic nanoparticles: applications and limitations. *Catalysts*. 2021;11(8):902. doi:10.3390/catal11080902
30. Javed R, Zia M, Naz S, Aisida SO, Ain NU, Ao Q. Role of capping agents in the application of nanoparticles in biomedicine and environmental remediation: recent trends and future prospects. *J Nanobiotechnology*. 2020;18(1):172. doi:10.1186/s12951-020-00704-4
31. Wang L, Zheng W, Li S, Zhong L, Jiang X. Aminophenol-Decorated Gold Nanoparticles for Curing Bacterial Infections. *Nano Lett*. 2022;22(9):3576–3582. doi:10.1021/acs.nanolett.1c04968
32. Huang Z, Liu H, Zhang X, et al. Ceftazidime-decorated gold nanoparticles: a promising strategy against clinical ceftazidime-avibactam-resistant Enterobacteriaceae with different resistance mechanisms. *Antimicrob Agents Chemother*. 2023;67(7):e0026223. doi:10.1128/aac.00262-23
33. Pierce VM, Bhowmick T, Simner PJ. Guiding antimicrobial stewardship through thoughtful antimicrobial susceptibility testing and reporting strategies: an updated approach in 2023. *J Clin Microbiol*. 2023;61(11):e0007422. doi:10.1128/jcm.00074-22
34. Xu M, Yao Z, Kong J, et al. Antiparasitic nitazoxanide potentiates colistin against colistin-resistant Acinetobacter baumannii and Escherichia coli in vitro and in vivo. *Microbiol Spectr*. 2024;12(1):e0229523. doi:10.1128/spectrum.02295-23
35. Liu H, Huang Z, Chen H, et al. A potential strategy against clinical carbapenem-resistant Enterobacteriaceae: antimicrobial activity study of sweetener-decorated gold nanoparticles in vitro and in vivo. *J Nanobiotechnology*. 2023;21(1):409. doi:10.1186/s12951-023-02149-x

36. Wistrand-Yuen P, Olsson A, Skarp KP, et al. Evaluation of polymyxin B in combination with 13 other antibiotics against carbapenemase-producing Klebsiella pneumoniae in time-lapse microscopy and time-kill experiments. *Clin Microbiol Infect*. 2020;26(9):1214–1221. doi:10.1016/j.cmi.2020.03.007
37. Chen -C-C, Lai -C-C, Huang H-L, et al. Antimicrobial activity of lactobacillus species against carbapenem-resistant Enterobacteriaceae. *Front Microbiol*. 2019;10:789. doi:10.3389/fmicb.2019.00789
38. Kong J, Wang Y, Yao Z, et al. Eugenol works synergistically with colistin against colistin-resistant Pseudomonas aeruginosa and Klebsiella pneumoniae isolates by enhancing membrane permeability. *Microbiol Spectr*. 2023;11(5):e0366622. doi:10.1128/spectrum.03666-22
39. Guo T, Sun X, Yang J, et al. Metformin reverse minocycline to inhibit minocycline-resistant Acinetobacter baumannii by destroy the outer membrane and enhance membrane potential in vitro. *BMC Microbiol*. 2022;22(1):215. doi:10.1186/s12866-022-02629-4
40. Cai J, Deng T, Shi J, Chen C, Wang Z, Liu Y. Daunorubicin resensitizes Gram-negative superbugs to the last-line antibiotics and prevents the transmission of antibiotic resistance. *iScience*. 2023;26(6):106809. doi:10.1016/j.isci.2023.106809
41. Zhang P, Ming Y, Cheng K, Niu Y, Ye Q. Gene expression profiling in ischemic postconditioning to alleviate mouse liver ischemia/reperfusion injury. *Int J Med Sci*. 2019;16(2):343–354. doi:10.7150/ijms.29393
42. Kanehisa M, Araki M, Goto S, et al. KEGG for linking genomes to life and the environment. *Nucleic Acids Res*. 2008;36(Database issue):D480–D484.
43. Pu S, Li J, Sun L, Zhong L, Ma Q. An in vitro comparison of the antioxidant activities of chitosan and green synthesized gold nanoparticles. *Carbohydr Polym*. 2019;211:161–172. doi:10.1016/j.carbpol.2019.02.007
44. Turakhia B, Chikkala S, Shah S. Novelty of bioengineered iron nanoparticles in nanocoated surgical cotton: a green chemistry. *Adv Pharmacol Sci*. 2019;2019:9825969. doi:10.1155/2019/9825969
45. Xie M, Gao M, Yun Y, et al. Antibacterial nanomaterials: mechanisms, impacts on antimicrobial resistance and design principles. *Angew Chem Int Ed Engl*. 2023;62(17):e202217345. doi:10.1002/anie.202217345
46. He J, Hong M, Xie W, Chen Z, Chen D, Xie S. Progress and prospects of nanomaterials against resistant bacteria. *J Control Release*. 2022;351:301–323. doi:10.1016/j.jconrel.2022.09.030
47. Nothling MD, Cao H, McKenzie TG, Hocking DM, Strugnell RA, Qiao GG. Bacterial redox potential powers controlled radical polymerization. *J Am Chem Soc*. 2021;143(1):286–293. doi:10.1021/jacs.0c10673
48. Zhong Y, Zheng XT, Zhao S, Su X, Loh XJ. Stimuli-activable metal-bearing nanomaterials and precise on-demand antibacterial strategies. *ACS Nano*. 2022;16(12):19840–19872. doi:10.1021/acsnano.2c08262
49. Mills E, O'Neill LAJ. Succinate: a metabolic signal in inflammation. *Trends Cell Biol*. 2014;24(5):313–320. doi:10.1016/j.tcb.2013.11.008
50. Peng B, Su Y-B, Li H, et al. Exogenous alanine and/or glucose plus kanamycin kills antibiotic-resistant bacteria. *Cell Metab*. 2015;21(2):249–262. doi:10.1016/j.cmet.2015.01.008
51. Stokes JM, Lopatkin AJ, Lobritz MA, Collins JJ. Bacterial Metabolism and Antibiotic Efficacy. *Cell Metab*. 2019;30(2):251–259. doi:10.1016/j.cmet.2019.06.009
52. Fan L, Pan Z, Liao X, et al. Uracil restores susceptibility of methicillin-resistant Staphylococcus aureus to aminoglycosides through metabolic reprogramming. *Front Pharmacol*. 2023;14:1133685. doi:10.3389/fphar.2023.1133685
53. Jiang M, Su Y-B, Ye J-Z, et al. Ampicillin-controlled glucose metabolism manipulates the transition from tolerance to resistance in bacteria. *Sci Adv*. 2023;9(10):eade8582. doi:10.1126/sciadv.ade8582
54. Huang X, Duan X, Li J, et al. The synergistic effect of exogenous glutamine and rifampicin against mycobacterium persisters. *Front Microbiol*. 2018;9:1625. doi:10.3389/fmicb.2018.01625
55. Chen Y-T, Ma Y-M, Peng -X-X, Li H. Glutamine potentiates gentamicin to kill lab-evolved gentamicin-resistant and clinically isolated multidrug-resistant Escherichia coli. *Front Microbiol*. 2022;13:1071278. doi:10.3389/fmicb.2022.1071278
56. Fan L, Pan Z, Zhong Y, et al. L-glutamine sensitizes Gram-positive-resistant bacteria to gentamicin killing. *Microbiol Spectr*. 2023;11(6):e0161923. doi:10.1128/spectrum.01619-23